Available online at www.sciencedirect.com

ScienceDirect

Geochimica et Cosmochimica Acta 157 (2015) 13–27

Geochimica et Cosmochimica Acta

www.elsevier.com/locate/gca

Mn–Cr dating of Fe- and Ca-rich olivine from 'quenched' and 'plutonic' angrite meteorites using Secondary Ion Mass Spectrometry

Seann J. McKibbin [a,b,*], Trevor R. Ireland [a], Yuri Amelin [a], Peter Holden [a]

[a] *Research School of Earth Sciences, Australian National University, Canberra, ACT, Australia*
[b] *Analytical, Environmental and Geo-Chemistry (AMGC), Vrije Universiteit Brussel, Brussels, Belgium*

Received 27 September 2014; accepted in revised form 12 February 2015; available online 21 February 2015

Abstract

Angrite meteorites are suitable for Mn–Cr relative dating (^{53}Mn decays to ^{53}Cr with a half life of 3.7 Myr) using Secondary Ion Mass Spectrometry (SIMS) because they contain olivine and kirschsteinite with very high ^{55}Mn/^{52}Cr ratios arising from very low Cr concentrations. Discrepant Mn–Cr and U–Pb time intervals between the extrusive or 'quenched' angrite D'Orbigny and some slowly cooled or 'plutonic' angrites suggests that some have been affected by secondary disturbances, but this seems to have occurred in quenched rather than in slow-cooled plutonic angrites, where such disturbance or delay of isotopic closure might be expected. Using SIMS, we investigate the Mn–Cr systematics of quenched angrites to higher precision than previously achieved by this method and extend our investigation to non-quenched (plutonic or sub-volcanic) angrites. High values of 3.54 ($\pm$0.18) $\times$ 10^{-6} and 3.40 ($\pm$0.19) $\times$ 10^{-6} (2-sigma) are found for the initial ^{53}Mn/^{55}Mn of the quenched angrites D'Orbigny and Sahara 99555, which are preserved by Cr-poor olivine and kirschsteinite. The previously reported initial ^{53}Mn/^{55}Mn value of D'Orbigny obtained from bulk-rock and mineral separates is slightly lower and was probably controlled by Cr-rich olivine. Results can be interpreted in terms of the diffusivity of Cr in this mineral. Very low Cr concentrations in Ca-rich olivine and kirschsteinite are probably charge balanced by Al; this substitutes for Si and likely diffuses at a very slow rate because Si is the slowest-diffusing cation in olivine. Diffusion in Cr-rich Mg–Fe olivine is probably controlled by cation vacancies because of deficiency in charge-balancing Al and is therefore more prone to disturbance. The higher initial ^{53}Mn/^{55}Mn found by SIMS for extrusive angrites is more likely to reflect closure of Cr in kirschsteinite at the time of crystallisation, simultaneous with closure of U–Pb and Hf–W isotope systematics for these meteorites obtained from pyroxenes. For the younger angrites Northwest Africa (NWA) 4590 and 4801 we have found initial ^{53}Mn/^{55}Mn values which are consistent with more precise work, at 0.90 ($\pm$0.4) $\times$ 10^{-6} and 0.13 ($\pm$1.1) $\times$ 10^{-6} respectively. Our work shows that SIMS can usefully constrain and distinguish the ages of angrites of different petrologic groups. In reviewing the petrology of angrites, we suggest that NWA 2999, 4590, and 4801 underwent a secondary partial melting and Cr (+/−Pb) disturbance event that the sub-volcanic Lewis Cliff 86010, and perhaps the plutonic Angra dos Reis, did not. With our higher initial ^{53}Mn/^{55}Mn for D'Orbigny and Sahara 99555 as well as previous data, a combined quenched angrite initial ^{53}Mn/^{55}Mn of 3.47 ($\pm$0.12) $\times$ 10^{-6} (2-sigma, MSWD 1.00) yields consistent Mn–Cr and U–Pb intervals between these angrites and Lewis Cliff 86010. Discrepant Mn–Cr timescales for other plutonic and sub-volcanic angrites represents resetting during the

* Corresponding author at: Research School of Earth Sciences, Bldg 61, Mills Rd, Acton 0200, Canberra, ACT, Australia. Tel.: +32 2629 1418; fax: +61 2 629 3391.

E-mail addresses: seann.mckibbin@gmail.com (S.J. McKibbin), trevor.ireland@anu.edu.au (T.R. Ireland), yuri.amelin@anu.edu.au (Y. Amelin), peter.holden@anu.edu.au (P. Holden).

http://dx.doi.org/10.1016/j.gca.2015.02.019
0016-7037/© 2015 Elsevier Ltd. All rights reserved.

secondary partial melting event at ~4557.2 Ma and indicates a relative order of disturbance of isotope systems: Mn–Cr in olivine before U–Pb in pyroxene, with Hf–W in pyroxene being the most resistant.
© 2015 Elsevier Ltd. All rights reserved.

1. INTRODUCTION

Angrites are evolved magmatic achondrite meteorites characterised by sub-basaltic SiO_2, a high CaO and FeO content (Mittlefehldt and Lindstrom, 1990; Mittlefehldt et al., 2002) with the latter reflecting a generally high oxidation state (approximately one log-unit above the iron–wustite oxygen fugacity buffer: Brett et al., 1977; McKay et al., 1994; Wadhwa, 2008) and a depletion of the alkali elements Na_2O and K_2O (Warren and Kallemeyn, 1995). While angrites are texturally diverse, some fall into a closely interrelated fine- to coarse-grained subgroup with strong crystal zoning often referred to as 'quenched', with bulk compositions controlled by olivine addition or removal and which crystallised from very similar magmas (Floss et al., 2003; Mikouchi et al., 2004). Their tightly grouped, unresolved ages obtained with multiple isotopic chronometers (Nyquist et al., 2003; Amelin, 2008a,b; Connelly et al., 2008; Spivak-Birndorf et al., 2009; Kleine et al., 2012) indicate that they may have been part of the same magmatic system. Other angrites are petrographically distinct in having equilibrated textures (Prinz et al., 1977; Treiman, 1989; Irving and Kuehner, 2007) and discrete, homogeneous olivine compositions often exhibiting exsolution lamellae of components either higher or lower in Ca (Mikouchi et al., 1995; McKay et al., 1998; Kuehner and Irving, 2007). These specimens do not seem to be so closely related to the quenched group or to each other, and multiple parent magmas are required to explain their compositions (Crozaz and McKay, 1990; Mittlefehldt et al., 2002). It is these characteristics, as well as their clearly resolved age differences (Brennecka and Wadhwa, 2012 recalculated after Amelin, 2008a; Kleine et al., 2012) that have led to the assignment of such angrites to a separate 'plutonic' grouping. The distinctive angrite geochemistry common to both quenched and plutonic angrites is suggestive of an origin in a single magmatic parent body, and this is supported by their oxygen isotopic compositions, which are related by mass-dependent fractionation processes (Greenwood et al., 2005).

The distinctive geochemistry of angrites is reflected in a unique mineralogical assemblage which make them suitable for dating using multiple isotopic decay schemes, especially the extant U–Pb system for which absolute ages can be obtained (Amelin, 2008a,b; Brennecka and Wadhwa, 2012), and the short-lived (now extinct) systems Mn–Cr (Lugmair and Shukolyukov, 1998; Glavin et al., 2004) and Hf–W (Kleine et al., 2012) with half lives of 3.7 and 8.9 Myr respectively (Honda and Imamura, 1971; Vockenhuber et al., 2004). The relatively large range of ages presented by angrites also provides an unparalleled opportunity for comparison and intercalibration of these dating systems. Comparison of Hf–W and U–Pb data has shown that angrite ages in these systems are generally consistent, with an interval of ~7 Myr having passed between crystallisation of the older quenched angrite D'Orbigny and isotopic closure in the youngest plutonic angrite Angra dos Reis (Kleine et al., 2012). However, the Mn–Cr timescale (recorded by Cr-isotope variations due to decay of ^{53}Mn to ^{53}Cr during the early history of the Solar System) is less well understood because of disagreement with the other isotope chronometers over the age interval between quenched angrites and one or more of the plutonic angrites (Amelin, 2008a). This implies that Mn–Cr ages are potentially low for the former or high for the latter, and could reflect slow cooling or secondary thermal resetting.

The history recorded by these meteorites over a very early period of Solar System and planetesimal evolution (4563.4 ± 0.3 to 4556.6 ± 0.3 Ma; Brennecka and Wadhwa, 2012) and their diverse geological origins therefore allow testing of the processes which affect diffusive closure of isotope systems in their respective mineral hosts. The Secondary Ion Mass Spectrometry (SIMS) analytical approach is useful for obtaining Mn–Cr ages for strongly zoned olivine and kirschsteinite in angrites (Sugiura et al., 2005) and can potentially unravel some of the microscale complexities in the Mn–Cr systematics of these meteorites. Additionally, because it involves minimal sample consumption, SIMS is suited to analysis of rare or small angrites when other techniques might be impractical. In this paper, we present SIMS Mn–Cr investigations of compositionally zoned olivine from the two largest quenched angrites D'Orbigny and Sahara 99555, and extend this approach to the more analytically challenging plutonic angrites Northwest Africa (NWA) 4590 and 4801 which contain unzoned olivine. This SIMS study was conducted in parallel with a Multi-Collector Inductively-Coupled-Plasma Mass-Spectrometry (MC-ICP-MS) study of the Mn–Cr chronology of these same angrites (Yin et al., 2009).

2. METHODS

2.1. 'Quenched' angrites D'Orbigny and Sahara 99555

To obtain Mn–Cr ages, complementary $^{53}Cr/^{52}Cr$ and $^{55}Mn/^{52}Cr$ information on a suite of co-genetic samples of the same age are required. In this SIMS study, the target materials are olivine grains analysed either in-situ in polished sections or as individual grains polished to expose their interiors. Chips of D'Orbigny and Sahara 99555 were obtained from the same specimens of these meteorites previously analysed by Amelin (2008a,b). They were mounted in epoxy and polished along with San Carlos olivine and synthetic olivine reference materials Mi6, Mi13 and Mi14 which were produced using experimental petrology techniques (McKibbin et al., 2013a). These olivines were also

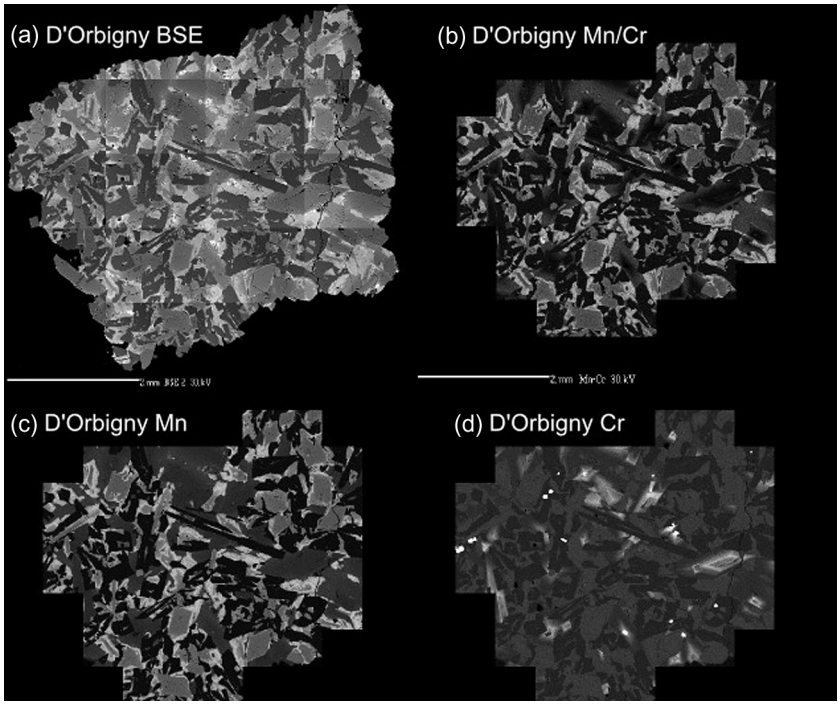

Fig. 1. Electron microprobe images of polished section of the quenched angrite D'Orbigny. (a) Back-scatter electron (BSE) image. Dark = anorthite; mid-tones = pyroxenes and Mg–Fe olivine cores; bright = Ca-rich olivine and kirschsteinite rims. (b) Mn/Cr elemental map. (c) Mn elemental map. (d) Cr elemental map.

used by McKibbin et al. (2013b) during work on the University of Tokyo piece of D'Orbigny previously analysed by Sugiura et al. (2005). Elemental mapping was undertaken on selected areas for Mn and Cr, combined with Back Scatter Electron (BSE) imaging to identify appropriate SIMS targets. X-ray elemental mapping was performed with a Cameca SX100 electron microprobe at the Research School of Earth Sciences, Australian National University and BSE imaging was performed on the same instrument or on a JEOL6400 Scanning Electron Microscope at the Centre for Advanced Microscopy at the Australian National University. In BSE images of D'Orbigny (Fig. 1a), medium and high intensities correspond to Mg–Fe and Fe–Ca olivine respectively, with midtones also representing pyroxene and dark areas representing anorthite. Our elemental maps show that the Mn/Cr ratio is clearly highest in olivine (Fig. 1b), with the Mg–Fe and Fe–Ca varieties having low and high values for this variable respectively, and therefore offering a wide range of Mn/Cr for in-situ SIMS analysis (Sugiura et al., 2005; McKibbin et al., 2013b). Mn/Cr ratio varies because of zoning in both elements. Mn in olivine is present at moderate concentrations in olivine cores, with higher Mn visible in discrete rims (Fig. 1c); this corresponds to a change in concentration by a factor of ~2–3 (~0.3–0.8 wt.% MnO; Mittlefehldt et al., 2002). D'Orbigny olivine is generally low in Cr (Fig. 1d); from dedicated electron probe microanalysis, Mittlefehldt et al. (2002) found Cr_2O_3 to be present at the level of ~0.04 wt.% in olivine cores and below detection limits in olivine rims. Pyroxene and small spinels are the main hosts of Cr, with strong zoning present in the former (Fig. 1d).

Sensitive High-mass-Resolution Ion Micro Probe Reverse Geometry (SHRIMP-RG) was used for in-situ measurement of isotopic ratios in D'Orbigny and Sahara 99555. Suitable areas ~20–30 μm in diameter were sputtered by a ~2–5 nA O_2^- primary ion beam (default SHRIMP operating conditions). Masses $^{52}Cr^+$, $^{53}Cr^+$ and $^{55}Mn^+$ were measured by adjusting the strength of the magnet and directing the ion beams sequentially into an electron multiplier. Mass resolution was adjusted to m/Δm ~5000–6000 (10% peak height) by use of a source slit (350 μm) and collector slit (350–500 μm) to resolve molecular interferences. The count rate for $^{55}Mn^+$ was kept below ~1 Mcps to minimise wear on the electron multiplier. Data collected over 10 magnet cycles (less than ~1000 s depending on setup conditions) were used in the ratio calculation in order to standardise temporal changes in observed $^{55}Mn^+/^{52}Cr^+$ associated with downhole effects as sputtering proceeded (discussed in McKibbin et al., 2013b).

SIMS data were reduced according to the 'first ratio estimator' method (Ogliore et al., 2011), which we have earlier referred to as 'Ratio of Total Counts' (McKibbin et al., 2013b), involving summing all data for each isotope from an analysis ($^{53}Cr^+$, $^{55}Mn^+$), and dividing by the sum of corresponding data for the normalising isotope for that analysis ($^{52}Cr^+$). Internal spot-specific errors were calculated as the standard error on the mean of sub-ratios determined for each magnet cycle within a single analytical spot. Instrumental mass fractionation (IMF) on Cr isotopes

was corrected by sample-standard bracketing with San Carlos olivine and a two-isotope correction procedure ($^{53}Cr/^{52}Cr$), assuming a 'terrestrial' value of 0.1134 for this reference material. Over six analytical sessions working on quenched angrites, we observed standard deviations of 3.5–8.2 permil on $^{53}Cr/^{52}Cr$ for reference grains.

The inter-element ratio $^{55}Mn^+/^{52}Cr^+$ has been shown to be susceptible to matrix effects in compositionally zoned olivine, predominantly the fayalite (Fe) content of olivine (McKibbin et al., 2013a) and was corrected by Mn–Cr relative sensitivity factors (RSF values). These have been determined by

$$RSF = (^{55}Mn/^{52}Cr)_{atomic}/(^{55}Mn^+/^{52}Cr^+)SIMS$$

and we use the same values of $(^{55}Mn/^{52}Cr)_{atomic}$ for our reference materials Mi6, Mi13 and Mi14 as reported in McKibbin et al. (2013b). The values for $(^{55}Mn^+/^{52}Cr^+)_{SIMS}$ were obtained under the same conditions as during the analytical sessions (including the same primary ion species) in which analyses of D'Orbigny and Sahara 99555 were made. As discussed in McKibbin et al. (2013b), the synthetic olivine compositions do not correspond precisely with the composition of the volume sampled during SIMS analysis of angrite olivine; further, zoning in angrite olivine could easily introduce percent-level bias to the final $^{55}Mn/^{52}Cr$ values. Therefore, in conjunction with the RSF values calculated for synthetic olivines in the current investigation, we have followed the methodology of McKibbin et al. (2013b) in determining olivine compositions at each SIMS crater using defocused quantitative SEM analysis and applied a least-squares mixing routine to find unique RSF values for each SIMS analysis as a function of the three chemical components in angrite olivine.

The slope of a regression of $^{55}Mn/^{52}Cr$ and $^{53}Cr/^{52}Cr$ data for olivine grains from each meteorite gives the abundance of the radioactive isotope ^{53}Mn with respect to the stable isotope ^{55}Mn at the time of isotopic closure or crystallisation, which we refer to as the initial $^{53}Mn/^{55}Mn$ for the meteorite. Similarly, regressions can be made for data on olivine from multiple meteorites or on bulk-rock data for several meteorites, in order to investigate the initial $^{53}Mn/^{55}Mn$ at the time of different fractionation events. All regressions were performed with the inverse-error weighting of points 'Model 1' function of Isoplot Ex. version 3.50 (Ludwig, 2006).

2.2. 'Plutonic' angrites NWA 4590 and 4801

Single mineral grains and grain aggregates of plutonic angrites NWA 4590 and 4801 were taken from the same specimens of these meteorites as analysed by Amelin and Irving (2007) and Amelin et al. (2011). Olivine was hand-picked and mounted along with mineral standards in epoxy. BSE imaging was undertaken to locate exsolution domains in olivine and kirschsteinite from NWA 4590 (Kuehner and Irving, 2007), which were the SIMS analytical targets, as well as mineral inclusions in olivine from NWA 4801, which were avoided.

Since plutonic angrites have, relative to the quenched angrites, lower initial $^{53}Mn/^{55}Mn$ and olivine with generally lower Mn/Cr (Lugmair and Shukolyukov, 1998; Glavin et al., 2004; Sugiura et al., 2005), we also present a variant of our method that is intended to achieve precision on Cr-isotopic analyses at the level of a few permil. Olivine and kirschsteinite from plutonic angrites were analysed by SHRIMP-II and SHRIMP-RG. In order to achieve higher count rates and higher precision, these analyses were conducted using a mixed composition (O^-, O_2^- and trace NO_2^-) primary beam to increase currents to ~17–53 nA while still sputtering relatively small (~30 micron) areas of the samples. Mass resolution was adjusted to m/Δm ~5000–6000 or better (10% peak height) by use of source and collector slits (350 μm and 350–500 μm respectively for SHRIMP-RG; 80 and 100 μm respectively for SHRIMP-II). An electron multiplier was used to collect $^{52}Cr^+$ on both instruments. Because of high primary sputtering beam currents, all beams were correspondingly more intense and the $^{55}Mn^+$ beam was too strong to be measured with an electron multiplier. $^{55}Mn^+$ was instead measured with a Faraday cup simultaneously with $^{52}Cr^+$ in the electron multiplier (SHRIMP-II multi-collector) or at another magnet setting and with deflection away from the electron multiplier and into the Faraday cup (SHRIMP-RG). $^{53}Cr^+$ was collected with the electron multiplier at another magnet setting on both instruments. Because of downhole variation in RSF during sputtering of each point (discussed in McKibbin et al., 2013b), a split run table was often employed, with the inter-element ratio $^{55}Mn^+/^{52}Cr^+$ being measured first, followed by $^{53}Cr^+/^{52}Cr^+$.

As for the quenched angrites, data reduction was conducted using the Ratio of Total Counts method and errors as the standard deviation of sub-ratios comprising each analysis. For San Carlos olivine, we again assumed a terrestrial $^{53}Cr/^{52}Cr$ of 0.1134 for the external IMF correction, finding standard deviations on this ratio of 0.6–4.3 permil over seven analytical sessions. The RSF values of the synthetic olivines were determined as for the quenched angrites, using the $(^{55}Mn/^{52}Cr)_{atomic}$ for our reference materials Mi6, Mi13 and Mi14 from McKibbin et al. (2013b). Values of $(^{55}Mn^+/^{52}Cr^+)_{SIMS}$ for reference materials were obtained under the same conditions and during the same analytical sessions as the analyses of NWA 4590 and 4801 olivine, with an unfiltered intense primary sputtering beam. The RSF mixing model was again applied; however, because olivine from plutonic angrites is not zoned, we used three discrete compositions and determined only three RSF values: one each for olivine and kirschsteinite from NWA 4590, and one for olivine from NWA 4801.

3. RESULTS

3.1. 'Quenched' angrites D'Orbigny and Sahara 99555

The RSF values we have calculated for our three synthetic olivine reference materials for use during analysis with filtered (O_2^-) and unfiltered (predominantly O_2^- and O^-) primary beams are below unity, and an increase in RSF occurs with increasing fayalite content. This is in accord with previous work on these materials (McKibbin et al., 2013b). RSF details are summarised in Table 1.

Table 1
Summary of relative sensitivity factors (RSF) for synthetic olivines used in this study (Fo, Fa, La and $(^{55}Mn/^{52}Cr)_{atomic}$ from McKibbin et al., 2013b).

Synthetic olivine	Mi6	Mi13	Mi14
Fo	0.5975	0.0472	0.0509
Fa	0.4021	0.7545	0.6147
La	0.0004	0.1982	0.3344
$(^{55}Mn/^{52}Cr)_{atomic}$	56.2	91.6	122.4
1 std. dev.	1.6	2.2	2.5
n	14	25	23
Filtered O_2^- primary beam for 'quenched' angrites			
$(^{55}Mn+/^{52}Cr+)_{SIMS}$	95.1	111.5	183.1
1 std. dev.	6.1	7.7	11.8
n	28	40	46
RSF	0.590	0.822	0.668
1-sigma	0.042	0.060	0.045
Unfiltered O_2^-, O^- primary beam for 'plutonic' angrites			
$(^{55}Mn+/^{52}Cr+)_{SIMS}$	90.6	119.5	177.9
1 std. dev.	4.3	7.8	8.2
n	17	9	9
RSF	0.620	0.766	0.688
1-sigma	0.035	0.053	0.035

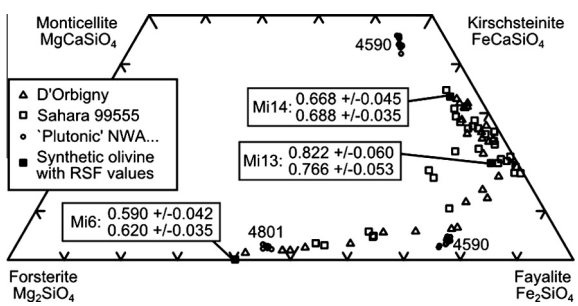

Fig. 2. Olivine ternary diagram illustrating the compositions of: synthetic olivine reference materials Mi6, Mi13 and Mi14; olivine corresponding to sputtered volumes during SIMS analysis of quenched angrites D'Orbigny and Sahara 99555, and plutonic angrites NWA 4590 and 4801. Synthetic olivines are labelled with RSF values for SIMS analytical sessions using a filtered primary beam (quenched angrites) and unfiltered primary beam (plutonic angrites).

Olivine compositions for the areas sputtered during SIMS analyses of D'Orbigny, Sahara 99555, NWA 4590 and NWA 4801 (Fig. 2; Electronic Appendix 1) are in general agreement with previously reported compositions (Mittlefehldt et al., 2002; Kuehner and Irving, 2007; Irving and Kuehner, 2007): Mg-rich olivine at $\sim Fo_{50-60}$ has the lowest Ca content, and Fe-rich olivine is progressively more enriched in Ca towards the kirschsteinite end-member. This is clearly seen in quenched angrite olivine which has a continuum of compositions. A couple of Sahara 99555 points with intermediate compositions at $\sim Fo_{16}$ Fa_{66} La_{18} (i.e. containing higher Ca for their Mg- and Fe-contents) may represent analytical mixtures of high- and low-Ca components that were not resolved by the poor spatial resolution of our defocused SEM analysis, which was intended to obtain an average composition for each sputtered area (Section 2.1). Plutonic angrites contain olivine of discrete compositions: olivine in NWA 4590 has exsolved into fayalitic and kirschsteinitic components, while NWA 4801 olivine is similar to that in the cores of the quenched angrites at $\sim Fo_{55}$.

Mn–Cr systematics obtained by SIMS reflect these diverse major element compositions for quenched angrites (Fig. 3 and Electronic Appendix 1; because Mn/Cr data for these angrites cover many orders of magnitude, we have used logarithmic axes for these meteorites). In D'Orbigny and Sahara 99555, $^{55}Mn/^{52}Cr$ ranges from lowest values of ~15–25 in olivine cores, to several million in Fe- and Ca-rich rims. In NWA 4590, $^{55}Mn/^{52}Cr$ is observed at two discrete values of ~400–900 for olivine, and ~2000–4000 for kirschsteinite exsolution lamellae. Olivine in NWA 4801 has a much smaller range of ~150–700, representing grain-to-grain variation. Cr-isotopic compositions are well correlated with Mn/Cr ratios in D'Orbigny, Sahara 99555 and NWA 4590. The initial $^{53}Cr/^{52}Cr$ (given by the intercept of the regression through $^{55}Mn/^{52}Cr$ and $^{53}Cr/^{52}Cr$ data) for D'Orbigny is 0.11325 (±0.00041; consistent with our assumed terrestrial value of 0.1134), and the initial $^{53}Mn/^{55}Mn$ is 3.54 (±0.18) × 10^{-6} (2-sigma, MSWD 0.74). Sahara 99555 is indistinguishable, at initial $^{53}Cr/^{52}Cr$ of 0.11369 (±0.00049; also consistent with terrestrial) and initial $^{53}Mn/^{55}Mn$ of 3.40 (±0.19) × 10^{-6} (2-sigma, MSWD 1.4). Isochron results are summarised in Table 2.

3.2. 'Plutonic' angrites NWA 4590 and 4801

At the better precision achieved during SIMS analysis with an unfiltered primary ion beam, different values of $^{53}Cr^+/^{52}Cr^+$ were resolved in each of the three synthetic olivines and the natural San Carlos and NWA meteoritic olivines. The raw $^{53}Cr^+/^{52}Cr^+$ from one of our SHRIMP II analytical sessions (uncorrected for IMF) are presented in Fig. 4 to illustrate this offset between samples (data given in Electronic Appendix 2). The variation might reflect a matrix effect of some kind, however, it is clear from Fig. 4 that it is not easily related to major element composition and that a relatively large residual discrepancy remains between olivine from NWA 4801 and Mi6 (~10 permil) or San Carlos (~15–20 permil). This was observed on both SHRIMP-RG and SHRIMP-II; such effects were not detected during our earlier investigation of D'Orbigny, which achieved precision on the initial $^{53}Cr/^{52}Cr$ of ~4 permil (McKibbin et al., 2013b), nor was it observed in this study on D'Orbigny and Sahara 99555. This matrix effect may represent a susceptibility of SHRIMP-geometry ion probes to unrecognised structural peculiarities of plutonic angrite (and other terrestrial and synthetic) olivines. Rather than attempt to correct for poorly understood effects, existing convention has been followed (e.g. Hutcheon et al., 1998; Hua et al., 2005; Hsu, 2005; Jogo et al., 2009; McKibbin et al., 2013b) and the external correction for IMF of Cr-isotopes has been carried out against San Carlos olivine. Because the residual IMF uniformly shifts $^{53}Cr/^{52}Cr$ to higher values, it does not seem to have affected the slope of the isochrons; useful initial $^{53}Mn/^{55}Mn$ constraints were still obtained.

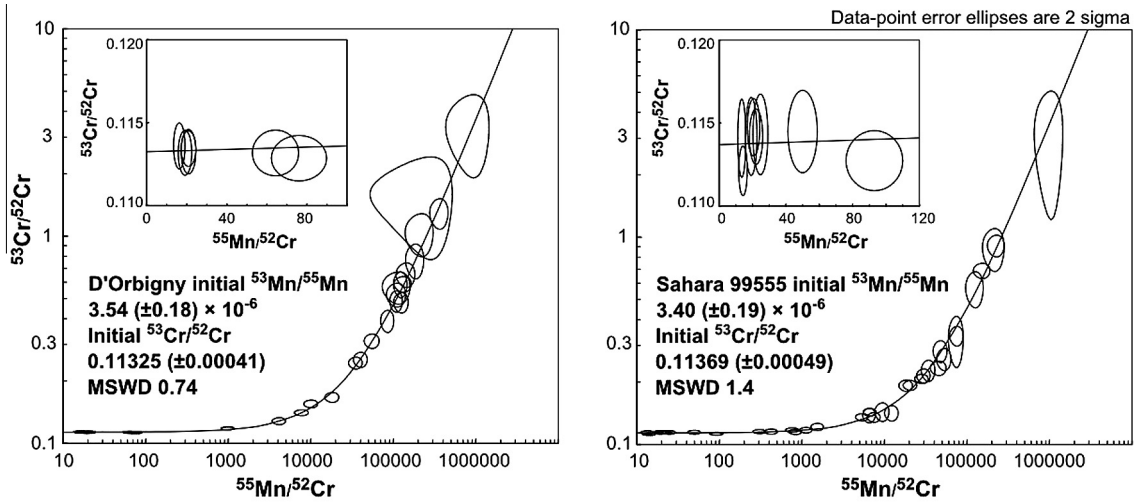

Fig. 3. SIMS Mn–Cr fossil isochrons for quenched angrites D'Orbigny and Sahara 99555. All data are shown in the main figures; in subfigures, the areas near the $^{53}Cr/^{52}Cr$ intercepts are shown. Both axes are logarithmic in the main figures and linear in subfigures. Error intervals are presented at the 2-sigma level.

Table 2
Summary of angrite initial $^{53}Cr/^{52}Cr$ and $^{53}Mn/^{55}Mn$ obtained by SIMS. Errors are 2-sigma except for the initial $^{53}Mn/^{55}Mn$ value for NWA 4801 which is presented at the 95% confidence level.

Meteorite	Initial $^{53}Cr/^{52}Cr$	Error	Initial $^{53}Mn/^{55}Mn$	Error	MSWD
D'Orbigny	0.11325	0.00041	3.54×10^{-6}	0.18×10^{-6}	0.74
Sahara 99555	0.11369	0.00049	3.40×10^{-6}	0.19×10^{-6}	1.4
NWA 4590	0.11465	0.00079	0.90×10^{-6}	0.4×10^{-6}	1.5
NWA 4801	0.11478	0.00037	0.13×10^{-6}	1.1×10^{-6}	3.4

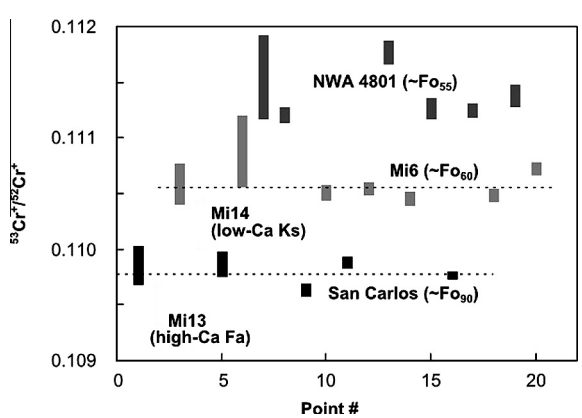

Fig. 4. Raw SIMS $^{53}Cr^{+}/^{52}Cr^{+}$ (uncorrected for IMF) for synthetic, natural terrestrial, and plutonic angrite olivine. Error bars are 1-sigma. Dotted lines indicate the inverse-error weighted means of San Carlos and Mi6 olivine.

The effect is a potentially higher initial $^{53}Cr/^{52}Cr$ for NWA 4590 of 0.11465 (±0.00079, near to the limit of terrestrial). Regression of Cr-isotopic data with Mn/Cr data gives an initial $^{53}Mn/^{55}Mn$ of 0.90 (±0.4) × 10^{-6} (2-sigma, MSWD 1.5) for this meteorite. For NWA 4801, because of our decision not to correct for the matrix effect, we have found a supra-terrestrial initial $^{53}Cr/^{52}Cr$ of 0.11478 (±0.00037) due to clear resolution of San Carlos olivine from the olivine in this meteorite. No correlation was observed between the inter-element ratio and isotopic composition of this meteorite; the initial $^{53}Mn/^{55}Mn$ is 0.13 (±1.1) × 10^{-6} (95% confidence, MSWD 3.4). Isochron results for plutonic angrites are illustrated in Fig. 5 and summarised along with quenched angrites in Table 2.

4. DISCUSSION

4.1. Initial $^{53}Mn/^{55}Mn$ of quenched angrites

In terms of relative ages, we have found D'Orbigny and Sahara 99555 to be unresolved from each other with similar initial $^{53}Mn/^{55}Mn$ values for both meteorites, in accord with previous SIMS work on their Mn–Cr systematics (Sugiura et al., 2005). However, our initial $^{53}Mn/^{55}Mn$ values are more precise, with relative errors of 5.1% and 5.6% respectively (at 95% confidence level and including full error estimates for RSF). This compares with their 2-sigma 'error-2' results (which includes a single systematic error estimate on the RSF), which are precise to a level of 8.5% and 13.1% respectively. Our results constrain the Mn–Cr age difference between these two meteorites to 0.22 ± 0.40 Myr, which is an improvement over the 0.04 ± 0.83 Myr obtained by Sugiura et al. (2005).

In absolute terms, our initial $^{53}Mn/^{55}Mn$ values of 3.54 (±0.18) × 10^{-6} and 3.40 (±0.19) × 10^{-6} for the quenched angrites D'Orbigny and Sahara 99555 are in agreement

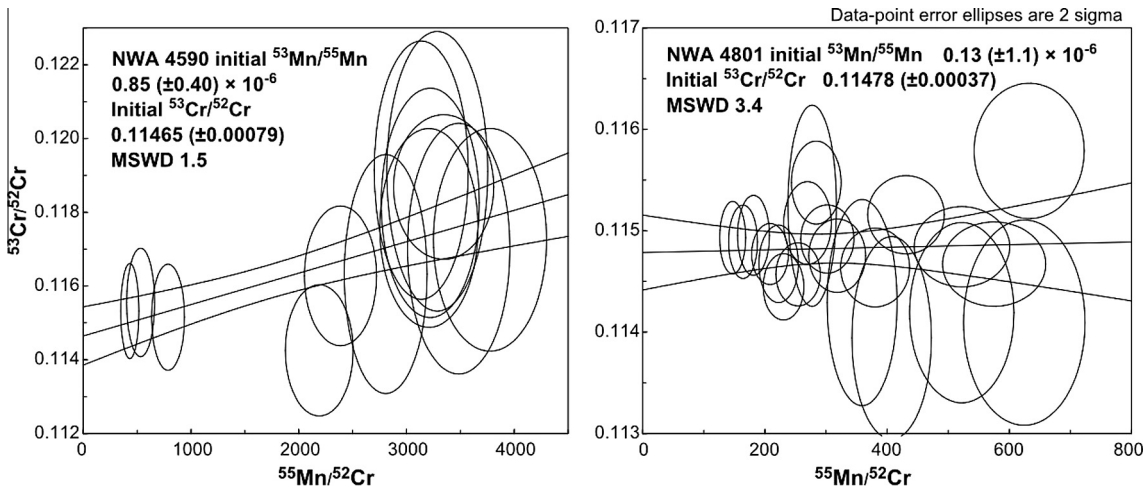

Fig. 5. SIMS Mn–Cr fossil isochrons for plutonic angrites NWA 4590 and NWA 4801. Errors are 2-sigma except for the initial $^{53}Mn/^{55}Mn$ for NWA 4801, which is presented at the 95% confidence level.

with our revised value found for the University of Tokyo chip of D'Orbigny (3.44 (±0.29) × 10^{-6}; McKibbin et al., 2013b), which used the same analytical method, including the same reference materials. Increased precision on the initial $^{53}Mn/^{55}Mn$ for D'Orbigny allows us to investigate potential discrepancy between SIMS and previous Thermal Ionisation Mass Spectrometry (TIMS) data. The new value for the University of Tokyo chip (McKibbin et al., 2013b) was consistent with the best initial $^{53}Mn/^{55}Mn$ of 3.24 (±0.04) × 10^{-6} found for D'Orbigny by Glavin et al. (2004) using TIMS. It was distinctly higher than the SIMS value of 2.84 (±0.24) × 10^{-6} from Sugiura et al. (2005), as well as the TIMS value of 2.83 (±0.25) × 10^{-6} from Nyquist et al. (2003). At the higher precision we have obtained here, our D'Orbigny initial $^{53}Mn/^{55}Mn$ value of 3.54 (±0.18) × 10^{-6} is resolved from the precise value of Glavin et al. (2004) for this meteorite. This is the case even if the stated error in that study only represents a 1-sigma interval (regression of their data using the Isoplot Ex. Model 1 regression yields an initial $^{53}Mn/^{55}Mn$ of 3.23 (±0.08) × 10^{-6} (2-sigma level, MSWD 3.3)). Hence we have another possible discrepancy between SIMS and TIMS values for D'Orbigny, with a higher SIMS value now apparent at the ~5% level.

Such a discrepancy is too large to represent a reasonable cosmogenic effect on Cr isotopes due to the short exposure histories of these meteorites, resulting in small isotopic effects (~parts per 10^4; Leya et al., 2003). They are very unlikely to be observable by SIMS and probably represent either analytical artifacts or a mineralogical effect. To evaluate possible discrepancies between SIMS and TIMS data, we now compare initial $^{53}Mn/^{55}Mn$ values of the quenched angrites D'Orbigny and Sahara 99555 with their RSF values. For each meteorite, an 'effective' RSF can be calculated from the ratio of the initial $^{53}Mn/^{55}Mn$ (i.e. our final, preferred values for initial $^{53}Mn/^{55}Mn$, which were found by regression of Cr-isotope and $(^{55}Mn/^{52}Cr)_{atomic}$ data) to the apparent initial $^{53}Mn/^{55}Mn$ regressed from Cr-isotope and $(^{55}Mn^+/^{52}Cr^+)_{SIMS}$ data before application of any

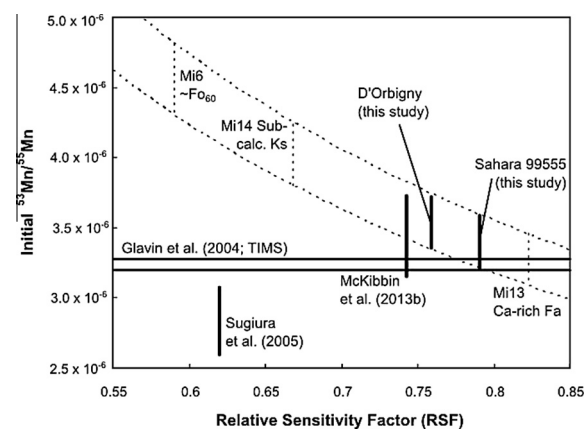

Fig. 6. Change of initial $^{53}Mn/^{55}Mn$ with relative sensitivity factor (RSF) for the results of this study for D'Orbigny and Sahara 99555 olivine-kirschsteinite compared with our reference materials and with previous studies. The 2-sigma error interval for our Sahara 99555 result is extrapolated across the RSF range; it is slightly larger than (although similar to) that of D'Orbigny. For comparison, confidence-limits on the high-precision Thermal Ionisation Mass Spectrometry (TIMS) determination of Glavin et al. (2004) are given as horizontal lines, as well as the Secondary Ion Mass Spectrometry (SIMS) studies of Sugiura et al. (2005) and McKibbin et al. (2013b) with their effective RSF values.

RSF. These effective RSF values will be similar to the mean or median of all RSF values used for each meteorite, but will also take into account the inverse-error weightings on each point applied by the Isoplot Ex. Model 1 regression. The apparent initial $^{53}Mn/^{55}Mn$, before RSF, for our determinations of D'Orbigny and Sahara 99555 are 2.69 (±0.14) and 2.69 (±0.23) × 10^{-6} respectively, giving effective RSF values of 0.759 and 0.791. For Sugiura et al. (2005), the effective RSF is simply their reported RSF, since only a single value was used in that study (0.62; because their D'Orbigny result is more than twice as precise as their Sahara 99555 result, we will consider only the former).

These data are presented in Fig. 6, along with errors on the TIMS value of Glavin et al. (2004) represented by horizontal lines. The change in initial $^{53}Mn/^{55}Mn$ with RSF is given by dotted lines for our Sahara 99555 result (for which the error envelope is slightly larger than that of D'Orbigny).

From our definition of RSF (Section 2.1) and from Fig. 6, it can be seen that use of higher RSF values in the mixing model would decrease the discrepancy, and move our initial $^{53}Mn/^{55}Mn$ for D'Orbigny to lower values. Systematic bias of our D'Orbigny effective RSF to values only a few percent lower could be an explanation for our finding, as might be illustrated by the location of Sahara 99555, at higher effective RSF and lower initial $^{53}Mn/^{55}Mn$, consistent with the TIMS result. However, in the current study, the RSF values we have found for Mi6, Mi13 and Mi14 using a filtered beam (0.590, 0.822 and 0.668 respectively) are already ~7–10% higher than for (McKibbin et al. (2013b); 0.552, 0.752 and 0.610 respectively). Arbitrary application of those lower RSF values would therefore increase the discrepancy. In our earlier study in which we developed the method for matrix-matched RSF values (McKibbin et al., 2013a), higher RSF values were indeed observed for the Fe–Mg olivine (~Fo_{60}, which included Mi6: RSF 0.62–0.63) and the 'low-Ca kirschsteinite', which included Mi14 (RSF 0.71), but a lower RSF was found for the 'high-Ca fayalite', which included Mi13 (RSF 0.75–0.77). It is therefore not clear whether such biases could resolve the discrepancy.

Regression of the new D'Orbigny data along with other samples does not change the initial $^{53}Mn/^{55}Mn$ much. Inclusion of data from McKibbin et al. (2013b) for the University of Tokyo piece (giving 3.51 ($\pm$0.16) $\times 10^{-6}$; MSWD 0.71), a combined D'Orbigny–Sahara 99555 regression of the data for both meteorites in this study (3.48 ($\pm$0.13) $\times 10^{-6}$; MSWD 1.11), or all three together (3.47 ($\pm$0.12) $\times 10^{-6}$; MSWD 1.00) all yield values clearly above that of Glavin et al. (2004). We have not resolved a difference between Sahara 99555 and the Glavin et al. (2004) value for D'Orbigny, which could be taken as support for the TIMS result, and is consistent with the strong dependence of accurate initial $^{53}Mn/^{55}Mn$ ratios on accurate RSF. However, the very good combined regression and the geochemical and petrological similarity of these meteorites suggests that a slightly higher initial $^{53}Mn/^{55}Mn$ for these meteorites bears geological meaning. These values are in agreement with the bulk-rock angrite Mn–Cr isochron reported by Shukolyukov and Lugmair (2007) of 3.40 ($\pm$0.14) $\times 10^{-6}$, and could be further evidence that crystallisation and cooling to diffusive closure of first-generation angrites occurred very shortly after differentiation of the angrite parent body, or contemporaneously with it, given our analytical uncertainties. In the next sections, we will explore potential mechanisms and implications of isotopic disturbance in D'Orbigny and other angrites.

4.2. Charge balancing of Cr in olivine and diffusive closure

We have made new determinations of the initial $^{53}Mn/^{55}Mn$ of quenched angrites, finding a difference of ~9% and a discrepancy (on the basis of 95% confidence limits) of ~2–3% between our SIMS result for D'Orbigny and the TIMS result of Glavin et al. (2004). Because unrecognised analytical biases only marginally explain this discrepancy, we will consider geochemical and mineralogical effects at the different levels of sampling (SIMS spot vs. whole mineral grains extracted for TIMS), and their possible influence on the isochron slope. All the SIMS Mn–Cr regressions for 'quenched' angrites are controlled largely by kirschsteinite and/or olivine with a considerable kirschsteinite component, with $^{55}Mn/^{52}Cr > 10^3$. In contrast, the regression of Glavin et al. (2004) is controlled by a combination of glass, total rock, and various olivine types with relatively low $^{55}Mn/^{52}Cr$ ratios of ~5–30, which from comparison with our analyses (Electronic Appendix 1) indicates that this olivine has an average composition of ~Fo_{60}. The difference between the new SIMS and the TIMS initial $^{53}Mn/^{55}Mn$ values (assuming that both values are accurate within their stated uncertainties) implies that diffusive closure of Cr was reached in Ca-rich olivine and kirschsteinite 0.47 ± 0.28 Myr before Mg–Fe olivine, or that secondary disturbance occurred in the latter. Ca-rich olivine and kirschsteinite in 'quenched' angrites is interstitial to other minerals or exists as rims on Mg–Fe olivine, and is one of the final crystallisation products of the angrite melt (Mittlefehldt et al., 2002; Kurat et al., 2004). Very Mg-rich 'xenolithic' olivine in angrites (up to ~Fo_{95}) is suggested to have been inherited from another part of the angrite parent body, and therefore to be older than the angrite groundmass (Mikouchi et al., 2011a) but this cannot be the case for small interstitial crystals or olivine rims. In the event of slow cooling or other later thermal disturbance, it might be expected that such thin rims and small interstitial crystals would be the most likely part of the rock to be affected, and that a lower initial $^{53}Mn/^{55}Mn$ would be found by SIMS analysis.

An investigation of charge-balancing and diffusion mechanisms for Cr in olivine provides a potential explanation. Cr is sensitive to oxygen fugacity and exists in silicate minerals as either Cr^{2+} or Cr^{3+} (e.g. Papike et al., 2005; Mallmann and O'Neill, 2009), with the latter likely dominating in angrites because of their high redox state (Brett et al., 1977; McKay et al., 1994).

Cr^{3+} substitutes for divalent Mg, Fe and Ca in the octahedral sites of olivine and maintains charge balance either by coupled substitution with another non-divalent element (Papike et al., 2005) or by a site vacancy. The preferred charge-balancing partner at low pressure is Al^{3+} (Taura et al., 1998) with the substitution proceeding according to $^{[VI]}Mg^{[VI]}Cr^{3+[IV]}Al^{3+}O_4$. In Ca-rich olivine and kirschsteinite in D'Orbigny, because of very low Cr content, Al is generally present in excess of charge balancing requirements, with Mittlefehldt et al. (2002) reporting 0.014–0.06 wt.% Al_2O_3 and maximum Cr_2O_3 contents of 0.004 wt.% (Kurat et al., 2004 report a single composition with sub-equal Al_2O_3 and Cr_2O_3 of 0.05 and 0.04 wt.% respectively). In contrast, Mg–Fe olivine shows more variable behaviour, with Kurat et al. (2004) reporting two olivines with Al/Cr ratios below unity (their 'Mega' and 'Rim' samples) and one above ('Core'), while Mittlefehldt et al. (2002) reports olivine with Fo_{64} and sub-equal Al_2O_3 and Cr_2O_3 of 0.07

and 0.043 wt.% respectively. This indicates that Ca-rich olivine and kirschsteinite with very low Cr concentrations (the main target of SIMS analysis) have excess of charge-balancing Al. In Cr-rich Mg–Fe olivine, the situation is often or generally reversed, with a vacancy mechanism occurring to greater or lesser degrees because of Al deficiency, and, in fact, because of deficiency in most other potentially trivalent trace elements as well (e.g. Ti, V, and Sc).

From elemental mapping of olivine in the more reduced pallasite meteorites (McKibbin et al., 2013c), a surplus of Cr involves some participation in charge-balancing with Al, but leaves a potentially divalent component free to diffuse. In that study, Cr records some older features also preserved by slowly diffusing trivalent Al, as well as more recent diffusion profiles also recorded by fast diffusing divalent Ni and Co. In contrast, a very small amount of oxidised Cr^{3+}, as occurs in angrite kirschsteinite, would imply that its residence in the crystal is controlled by Al. Excess Al can charge balance itself by occupying both octahedral and tetrahedral sites according to $Mg^{[VI]}Al^{3+[IV]}Al^{3+}O^{4}$ (Evans et al., 2008); on the other hand, Cr^{3+} does not occupy the tetrahedral site (Burns, 1975) and presumably cannot charge balance itself in this manner. With trace amounts of Cr substituted into Ca-rich olivine and kirschsteinite according to $^{[VI]}Mg^{[VI]}Cr^{3+[IV]}Al^{3+}O_4$, the diffusion of Cr is also likely to be reliant on Al, which can be very slow (Spandler and O'Neill, 2010). High concentrations of Cr^{3+} in more Mg- and Fe-rich angrite olivine is likely to be charge balanced by vacancies because of the deficiency in other trivalent cations. In this situation, the diffusion of Cr is likely to be faster. Thus, there is a crystal-chemical basis to expect that high-Ca olivine and kirschsteinite with Al > Cr might be closed to Cr diffusion while Mg–Fe olivine with Al < Cr is not, and that the former could be more resistant to thermal disturbance than the latter.

Though there is no obvious petrologic evidence for a late disturbance in quenched angrites, conflicting results have been presented for Sm–Nd by Tonui et al. (2003) and Sanborn et al. (2011). Further studies of anorthite may shed light on the situation, because of its sensitivity to resetting of Mg isotopes and as suggested by these studies possibly also Nd isotopes. If the diffusivity of vacancy-mediated Cr^{3+} in Mg–Fe olivine is similar to divalent cations such as Mg, Fe, Ca and Ni, as has been shown to be possible under certain experimental conditions involving Al < Cr (Spandler and O'Neill, 2010), then slight disturbance of olivine could occur during more moderate or severe disturbance of anorthite. For example, at near-solidus temperatures, the diffusivity of Mg in plagioclase or anorthite (Latourrette and Wasserburg, 1998; Faak et al., 2013) is probably 1–2 orders of magnitude faster than that of divalent elements in olivine (e.g. Petry et al., 2004; Spandler and O'Neill, 2010), 3–4 orders of magnitude faster than Cr in olivine (as a mixture of divalent and trivalent Cr; Ito and Ganguly, 2006), and more than 8 orders of magnitude faster than Si in olivine (Dohmen et al., 2002). Trace elements substituting into the olivine tetrahedral site, such as Al, probably diffuse slowly in a manner similar to Si. Because of the likely charge-balancing interactions between slow-diffusing Al and trivalent Cr in Ca-rich olivine and kirschsteinite, we suggest that the Mn–Cr systematics of D'Orbigny and Sahara 99555 have been better preserved by these phases because they have Al > Cr. The potential sensitivity of anorthite to disturbance suggests that further study of this mineral, particularly utilising the Al–Mg and Sm–Nd systems and addressing microscale distribution of these elements, might indicate whether, and to what level, D'Orbigny and other angrites have been disturbed.

4.3. Petrology and initial $^{53}Mn/^{55}Mn$ of plutonic angrites

For most of the younger 'plutonic' angrites, there is clear petrographic and geochemical evidence for slower cooling and in some, late thermal or melting events. The Lewis Cliff (LEW) 86010 and NWA 4590 angrites contain chemically zoned pyroxenes, with clear Mg-rich cores and irregular zoning in the former, but also contain compositionally homogeneous olivine with exsolved kirschsteinite lamellae of discrete compositions, in strong contrast to the zoned olivine in quenched angrites (Goodrich, 1988; McKay et al., 1988; Kuehner and Irving, 2007). This requires a relatively slow-cooling environment, with quantitative estimation of cooling rates from subtle Ca-zoning adjacent to kirschsteinite lamellae in LEW 86010 indicating that most of the exsolution took place below 1273 K, and cooling to ambient temperature occurred over ~10–250 years at a depth of <100 m (McKay et al., 1998). While homogeneous olivine compositions clearly indicate slower cooling than the quenched angrites, for the purposes of isotopic dating, the plutonic angrite LEW 86010 is in fact just as suitable for a chronological 'anchor' as the older angrites D'Orbigny, Sahara 99555 and their relatives. Considering the estimated cooling rates, rather than representing a truly deep-seated plutonic angrite, LEW 86010 might be better thought of as a 'sub-volcanic' rock.

The textural and crystal-chemical similarity of NWA 4590 to LEW 86010 are consistent with a comparable fast-cooling history for the former. Cooling rate estimates have been undertaken on the lamellae in NWA 4590, finding that this meteorite cooled ~10 times slower than LEW 86010, corresponding to a depth of ~240 m (Mikouchi et al., 2011b); this also implies effectively instantaneous closure of relevant short-lived nuclide decay systems. However, other petrologic evidence indicates that NWA 4950 is not as pristine as LEW 86010. Kuehner and Irving (2007) observed grain-boundary glasses with a composition intermediate to anorthite and ulvöspinel, together with secondary kirschsteinite, clinopyroxene and olivine. This glass was reported to crosscut kirschsteinite lamellae, and was interpreted to be a product of decompression melting during exhumation. However, such an interpretation seems in conflict with the considerable cooling required to intersect the olivine-kirschsteinite solvus (Mukhopadhyay and Lindsley, 1983) before melting; return to the solidus via re-heating, without the involvement of pressure, might be a simpler explanation. Further evidence for disturbance in NWA 4590 comes from distinct U–Pb ages for phosphates, which closed to Pb diffusion 0.55 ± 0.29 My after Pb in pyroxenes (Amelin et al., 2011; Amelin and Sapah,

2012; assuming the same $^{235}U/^{238}U$ for each phase). This was interpreted to reflect slow cooling in a plutonic environment with an inferred cooling rate of several hundred K per Myr. Alternately, NWA 4590 phosphates could date the secondary partial melting event which resulted in the formation of glass, or could represent a disturbed age, especially considering that P is one of the first elements to be mobilised during eutectic partial melting of phosphate-bearing silicate rocks (Yamaguchi et al., 2013). Again, rather than representing a truly 'plutonic' angrite, the zoning in pyroxene and exsolution lamellae in olivine suggests that NWA 4590 is similar to LEW 86010 in having formed in a sub-volcanic environment, perhaps cooling over less than a few thousand years. Additionally, NWA 4590 may record a secondary melting event resulting in low-degree eutectic partial melting and resetting of U–Pb systematics in phosphates ~0.5 Myr after crystallisation.

Other angrites do seem to be genuinely slow-cooled plutonic rocks. The lack of chemical variation in both pyroxene and olivine from Angra dos Reis, NWA 2999, and NWA 4801 (Prinz et al., 1977; Kuehner et al., 2006; Irving and Kuehner, 2007) indicates much lower cooling rates than LEW 86010 and NWA 4590, or possibly much longer secondary thermal perturbations. Additionally, the anhedral texture of NWA 4801 has been interpreted as reflecting a history of high-temperature annealing (Irving and Kuehner, 2007). As for NWA 4590, unusual features of secondary origin are also present in NWA 2999 including radial symplectic pyroxene-spinel intergrowths between anorthite and olivine porphyroclasts, and anorthite coronas on spinel grains in contact with pyroxene (Kuehner et al., 2006). No such features have been reported in Angra dos Reis or NWA 4801.

Our SIMS investigation of the initial $^{53}Mn/^{55}Mn$ of plutonic angrites has yielded values of 0.90 (±0.4) × 10^{-6} and <1.23 × 10^{-6} for NWA 4590 and 4801 respectively. These are in agreement with higher precision MC-ICP-MS and TIMS work on these meteorites which found 1.01 (±0.12) × 10^{-6} (Yin et al., 2009) and 1.00 (±0.07) × 10^{-6} respectively (Shukolyukov et al., 2009). They are similar to the slightly higher value of 1.25 (±0.07) × 10^{-6} for LEW 86010 and the less precise values of 1.1 (±0.4) × 10^{-6} for Angra dos Reis (Lugmair and Shukolyukov, 1998) and 1.28 (±0.23) × 10^{-6} for NWA 2999 (Shukolyukov and Lugmair, 2008). While our results are not sufficiently precise to resolve these fine-scale initial $^{53}Mn/^{55}Mn$ variations in these meteorites, our method provides an efficient alternative to bulk techniques in determining approximate initial $^{53}Mn/^{55}Mn$ values and is capable of clearly resolving first-generation quenched angrites from later generation plutonic or sub-volcanic angrites. To resolve angrite initial $^{53}Mn/^{55}Mn$ from zero using SIMS, a mineral with high Mn/Cr such as kirschsteinite is required; in the absence of such a phase, only upper limits on initial $^{53}Mn/^{55}Mn$ can reasonably be achieved. If, in the future, new plutonic 'mini-angrites' were to be discovered (e.g. of a size comparable to the quenched angrite LEW 87051 at 0.6 g; McKay et al., 1990), SIMS will be able to provide useful initial $^{53}Mn/^{55}Mn$ values. Some issues remain with initial $^{53}Cr/^{52}Cr$ of plutonic angrites due to the poorly understood matrix effect we chose not to correct for (Section 3 and Fig. 4), especially for the higher precision measurements on NWA 4801, and might be related to excess scatter we obtained for this meteorite (MSWD 3.4).

In our previous study of D'Orbigny, we presented a comparison of the initial $^{53}Mn/^{55}Mn$ of non-quenched angrites with their pyroxene U-Pb ages (Fig. 9 in McKibbin et al., 2013b) in which it can be seen that LEW 86010 has, for a U–Pb age similar to that of NWA 4590 and 4801, a distinctly higher initial $^{53}Mn/^{55}Mn$. Use of more precise phosphate U–Pb ages for NWA 4590 instead of pyroxene ages do not bring this meteorite closer to an initial $^{53}Mn/^{55}Mn$ and U–Pb evolution line passing through LEW 86010, since they are only ~0.5 Myr younger (Amelin et al., 2011; Amelin and Sapah, 2012). The initial $^{53}Mn/^{55}Mn$ ratios of the non-quenched angrites are controlled by various mineral phases: olivine for LEW 86010; olivine and pyroxene for NWA 4590; pyroxene for NWA 4801 (referred to originally as 'olivine' but with a much lower $^{55}Mn/^{52}Cr$ ratio than we have found); and total rock/silicate components for NWA 2999 (Lugmair and Shukolyukov, 1998; Yin et al., 2009; Shukolyukov et al., 2009; Shukolyukov and Lugmair, 2008 respectively).

In light of the petrology of these meteorites, which indicate that the latter three were disturbed by a secondary melting or slow cooling event resulting in annealed textures, secondary glasses, symplectic pyroxene-spinel intergrowths, and anorthite coronas on spinel grains, it seems that the higher initial $^{53}Mn/^{55}Mn$ of LEW 86010 could reflect its pristine nature and it might be a better sample of the late isotopic evolution of the angrite parent body. The difference in initial $^{53}Mn/^{55}Mn$ between this meteorite and our SIMS value for Ca-rich olivine and kirschsteinite in D'Orbigny corresponds to 5.62 ± 0.48 Myr; in agreement with the U–Pb age difference of 5.86 ± 0.19 Myr (Amelin, 2008a). This resolves a previous discrepancy between Mn–Cr and U–Pb timescales in angrites, with the difference between the initial $^{53}Mn/^{55}Mn$ values for LEW 86010 (Lugmair and Shukolyukov, 1998) and D'Orbigny as found by Glavin et al. (2004) representing only 5.14 ± 0.39 Myr. As discussed in Section 4.2, the discrepancy could reflect disturbance of Cr-rich Mg–Fe olivine in D'Orbigny while radiogenic Cr in Ca-rich olivine and kirschsteinite was better retained due to charge balancing with Al.

With this view that the high SIMS initial $^{53}Mn/^{55}Mn$ values for quenched angrite olivine-kirschsteinite are more likely to correspond to crystallisation ages and hence to U–Pb ages obtained from pyroxenes for these meteorites, such an anchor point can be used to construct a Mn–Cr and U–Pb (as well as Hf–W) history for the angrite parent body. Taking meteorite petrology and indicators of isotopic disturbance into account, and guided by the observation that of the non-quenched angrites, only LEW 86010 is likely to have Mn–Cr and U–Pb systematics which closed simultaneously (and for which data of high enough precision are available), an improved geological history can be drafted. The most robust interpretation of the Mn–Cr systematics of quenched angrites is likely to be based on the combined D'Orbigny–Sahara 99555 isochron, including points from McKibbin et al. (2013b), which gives an initial

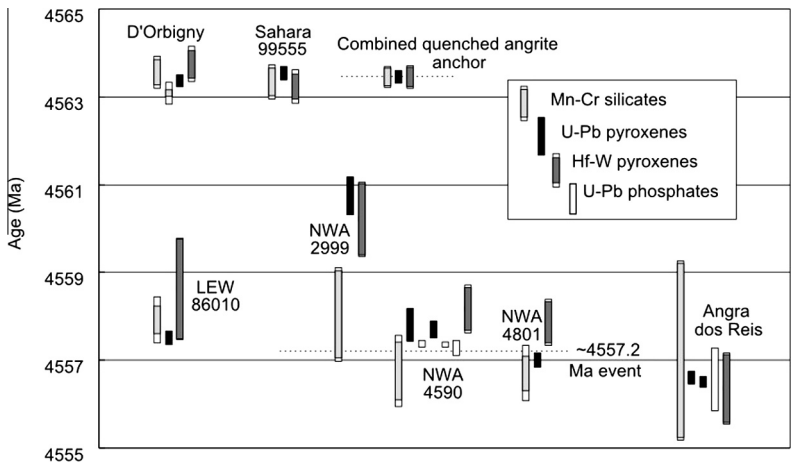

Fig. 7. Mn–Cr, U–Pb and Hf–W timescales for angrite meteorites. Relative chronometers are anchored to combined 'quenched angrite' isochrons. Two errors are presented for relative chronometers: the smaller indicating purely analytical errors for comparison within a single isotope system; the larger including analytical error for the anchor of that decay system, error on the relative chronometer half-life, and error on the absolute U–Pb age of the anchor. Original Mn–Cr data from: Lugmair and Shukolyukov (1998), Glavin et al. (2004), Shukolyukov and Lugmair (2008), Shukolyukov et al. (2009), Yin et al. (2009); and this study. Original U–Pb–Pb data from: Amelin and Irving (2007), Amelin (2008a), Connelly et al. (2008), Amelin et al. (2011), Amelin and Sapah (2012), Brennecka and Wadhwa (2012). Original Hf–W data from: Kleine et al. (2012). The data and are summarised in Electronic Appendix 3).

$^{53}Mn/^{55}Mn$ of 3.47 $(\pm 0.12) \times 10^{-6}$ (MSWD 1.00) (Section 4.1). An equivalent isochron for the Hf–W system was determined by Kleine et al. (2012) using D'Orbigny and Sahara 99555 data, at initial $^{182}Hf/^{180}Hf$ of 6.99 $(\pm 0.11) \times 10^{-5}$. These can be anchored to the mean of D'Orbigny and Sahara 99555 U–Pb ages at 4563.46 ± 0.13 (Connelly et al., 2008; Amelin, 2008a), corrected for the angrite $^{238}U/^{235}U$ composition (Brennecka and Wadhwa, 2012). We have not included the error on the $^{238}U/^{235}U$ ratio in the error propagation since U-isotopes were probably homogenised during planetary differentiation. In Fig. 7, we plot U–Pb ages with Mn–Cr and Hf–W ages calculated relative to this anchor.

Two types of errors are shown in Fig. 7, with the smaller representing purely analytical errors on short-lived isotope ages (for comparison within a single isotope system, e.g. between D'Orbigny Mn–Cr data obtained by SIMS and TIMS), and the larger the total propagated error including errors on the anchor initial $^{53}Mn/^{55}Mn$ or $^{182}Hf/^{180}Hf$, as well as error on the U–Pb age of the anchor, and error on the half-lives of ^{53}Mn and ^{182}Hf. For ^{53}Mn, we use a half-life of 3.76 ± 0.24 Myr, which represents an inverse-error weighted mean of the values reported by Matsuda et al. (1971); 2.9 ± 1.2 Myr, Honda and Imamura (1971); 3.7 ± 0.4 Myr), Woelfle et al. (1973); 3.9 ± 0.6 Myr, Herr et al. (1972); 3.8 ± 0.7 Myr, and Heimann et al. (1974); 3.85 ± 0.4 Myr. It should be noted that the weighted mean is rather insensitive to which or how many of these studies are included in the calculation, and the influence on angrite chronology is subtle. For ^{182}Hf we use the precise value of 8.90 ± 0.17 Myr from Vockenhuber et al. (2004). As expected from the petrologic investigations, LEW 86010 exhibits consistent U–Pb pyroxene, Hf–W pyroxene, and Mn–Cr olivine ages when the latter are anchored to the combined quenched-angrite age. All isotope systems are also in agreement for Angra dos Reis, although in this case the poorer reported precision for Mn–Cr in silicate, U–Pb in phosphate, and Hf–W in pyroxene makes these ages insensitive to possible disturbances. Other non-quenched angrite ages exhibit varying levels of discrepancy. The Mn–Cr total rock/silicate age for NWA 2999 is clearly younger than U–Pb and Hf–W pyroxene ages for this meteorite. In NWA 4590, there is potentially better agreement of olivine-pyroxene Mn–Cr with phosphate U–Pb than with pyroxene U–Pb. Hf–W in pyroxene also seems to indicate dispersion in this meteorite, since it is higher than phosphate ages and perhaps only marginally in agreement with Mn–Cr. NWA 4801 also exhibits discordance, although here discrepancy between U–Pb and Hf–W ages is prominent, with the former in better agreement with Mn–Cr and the latter recording an older age. The general trend of discordance indicates that Mn–Cr in silicates (i.e. pyroxene–olivine mixtures) is more easily reset than U–Pb in pyroxenes. This is in agreement with current understanding of the diffusivities of Cr in olivine and Pb in pyroxene (reviewed in Amelin, 2008a). U–Pb in phosphates may be reset at an intermediate stage, as implied by the agreement between U–Pb and Hf–W ages for pyroxene in NWA 4590 but younger ages for the phosphates. Hf–W in pyroxene may be the most resistant, with ages in agreement with U–Pb in pyroxene in all cases except for NWA 4801, in which it is older.

Discordance in NWA 2999 and NWA 4801, as well as potentially better agreement between Mn–Cr in silicates and U–Pb in phosphates for NWA 4590, are suggestive of a secondary event which set the Mn–Cr systematics at some time after U–Pb and/or Hf–W closure in pyroxenes. The possible match between Mn–Cr in silicates and U–Pb in phosphates for NWA 4590 is consistent with this event being the partial melting that resulted in symplectite and coronal features in these meteorites. Two end-member

scenarios can be considered to interpret such age differences: (1) If this disturbance resulted in complete resetting of Mn–Cr systematics in olivine and pyroxene, as seems possible for a low-degree partial melting event, then after decay of ^{53}Mn the observed initial ^{53}Mn/^{55}Mn of these meteorites would record the timing of the disturbance directly; (2) If the disturbance did not reset the Mn–Cr systematics at all, then the initial ^{53}Mn/^{55}Mn should record the same age as U–Pb or Hf–W in pyroxene as though nothing occurred, i.e. with the same outcome as for LEW 86010. An intermediate situation would involve partial resetting of Mn–Cr (and perhaps U–Pb) systematics, which would after decay of ^{53}Mn yield an intermediate initial ^{53}Mn/^{55}Mn and give only an upper limit on the age of the disturbance. Such a disturbance might have occurred very much later. The low U–Pb age of NWA 4801 pyroxene, and an intermediate U–Pb age of NWA 4590 phosphates, may indicate a similar situation for this isotope system. Nevertheless, the general agreement between the Mn–Cr ages of NWA 4590, NWA 2999, and NWA 4801 implies complete resetting of Cr-isotopes in these rocks, as well as partial disturbance of phosphate U–Pb in the former and partial or complete disturbance of pyroxene U–Pb in the latter. These characteristics seem to date the same partial melting and disturbance event which occurred at ~4557.2 Ma.

It is important to note that even if our high initial ^{53}Mn/^{55}Mn for the quenched angrite, D'Orbigny, can be attributed to analytical bias, then the history we have outlined is not particularly affected because it relies on high-precision data for the non-quenched angrites, and incorporates important petrologic observations about them. It is, however, clear from Fig. 7 that data for Angra dos Reis are especially limiting, and if they could be improved then the history presented here could be precisely tested. Additionally, some limitation is imposed by the knowledge of the ^{53}Mn half life, which if better constrained would slightly improve the situation for the more precisely determined angrite Mn–Cr ages.

In analysing such a planetary history, it is important to recognise two different but complementary philosophical approaches used to develop short-lived isotope chronologies. Selection of an appropriate anchor point for the Mn–Cr and Hf–W relative histories can be attempted on the basis of data obtained from a single (or combined) meteoritic sample, as is the case here; alternately, it can be achieved by regression of data from two isotope systems for many meteorites (as in Kleine et al., 2012). The former involves selection of an isotopically representative sample and identifies whether other samples are consistent with the evolution of that source, while the second seeks overall consistency and averages out many geological effects. For example, one could, within errors, shift the entire Mn–Cr timescale in Fig. 7 upwards to achieve better concordance for NWA 4590 and NWA 4801 (as would be the case if the initial ^{53}Mn/^{55}Mn for D'Orbigny from Glavin et al., 2004 was used as the anchor), but after a certain point, discrepancy with LEW 86010 would appear. Similarly, the Hf–W timescale could be shifted downwards to achieve better agreement for these meteorites, but discrepancy would soon be observed in Sahara 99555. Guided by the petrology of these rocks, it should be possible to come to a geologically reasoned best-fit, rather than a solution driven by a search for consistency which may not actually exist. In doing so, and obviously with recognition of and careful correction for laboratory biases, the resolution of inconsistency between chronometers yields geological information. This kind of information, including the timing of differentiation, crystallisation, diffusive isotopic closure, secondary partial melting, and other disturbances, is an important goal of extant- and extinct-nuclide investigations of early Solar System rocks.

5. CONCLUSIONS

Re-investigation of angrite Mn–Cr systematics using SIMS at higher precision than previously achieved by this method has found values for the initial ^{53}Mn/^{55}Mn of quenched angrites that are higher than obtained by TIMS (Glavin et al., 2004), at 3.47 ($\pm$0.12) $\times 10^{-6}$ (2-sigma, MSWD 1.00) for a combined D'Orbigny–Sahara 99555 isochron, including some previous SIMS data (McKibbin et al., 2013b). In our investigation, the slopes of Mn–Cr isochrons are controlled by Ca-rich olivine or kirschsteinite, whereas in TIMS work the isochrons are generally controlled by Mg–Fe olivine, pyroxene, or mixtures. Cr^{3+} in the octahedral site in Ca-rich olivine or kirschsteinite is probably charge-balanced by Al^{3+} in the tetrahedral site. Since tetrahedrally sited cations such as Si and probably Al are the slowest-diffusing species in olivine, we suggest that an excess of Al (Cr < Al) enabling charge-balancing of Cr will lead to very low diffusivities for the latter, with a higher effective closure temperature and greater resistance to thermal resetting. Cr in Mg–Fe olivine is present in excess relative to Al (Cr > Al), and diffusion is probably vacancy-mediated and therefore relatively fast. SIMS analysis might therefore have identified a Cr-component more likely to have been set at the time of crystallisation, and which can be used as an alternate Mn–Cr anchor for inter-comparison with U–Pb and Hf–W timescales. Our value for the initial ^{53}Mn/^{55}Mn of quenched angrites is in agreement with the bulk-rock Mn–Cr fossil isochron obtained for these meteorites (Shukolyukov and Lugmair, 2007) implying rapid cooling of extrusive crust immediately after mantle-crust differentiation in the angrite parent body. Our value also resolves some outstanding discrepancies between Mn–Cr, U–Pb and Hf–W timescales, indicates a relative disturbance order (Mn–Cr in olivine before U–Pb in pyroxene, with Hf–W in pyroxene being the most resistant), and is more consistent with the geologic history of quenched and non-quenched angrites as inferred from petrographic investigations. Extension of SIMS analysis to the plutonic angrites brings microscale Mn–Cr investigations to these meteorites for the first time, allowing for the possibility of age investigations on plutonic 'mini-angrites' in the event they are found. For SIMS analysis, kirschsteinite is required to obtain Mn–Cr isochrons with slopes resolved from zero, but useful upper limits can be obtained even without analysis of this mineral.

ACKNOWLEDGEMENTS

We thank John Fitzgerald, Robert Rapp and Ashley Norris for assistance with sample preparation and EMPA analysis, and Charlotte Allen and Guil Mallmann for discussion of LA-ICP-MS data. This study benefited from many discussions with Peter Lanc, Tanya Ewing, Janaina Avila, Ian Williams and Ingo Leya. The Australian National University Centre for Advanced Microscopy provided technical support and access to SEM facilities. Meenakshi Wadhwa generously provided angrite samples for this study. We thank Christine Floss and two anonymous reviewers for their constructive criticisms, and Maud Boyet for editorial handling. This research was supported by grants DP034277 and DP0666751 from the Australian Research Council to TRI and YA, and an Australian National University PhD Research Scholarship. SMcK is currently a postdoctoral fellow of the Research Foundation-Flanders (FWO).

APPENDIX A. SUPPLEMENTARY DATA

Supplementary data associated with this article can be found, in the online version, at http://dx.doi.org/10.1016/j.gca.2015.02.019.

REFERENCES

Amelin Y. (2008a) U-Pb ages of angrites. *Geochim. Cosmochim. Acta* **72**, 221–232.

Amelin Y. (2008b) The U-Pb systematics of angrite Sahara 99555. *Geochim. Cosmochim. Acta* **72**, 4874–4885.

Amelin Y. and Irving A. J. (2007) Seven million years of evolution on the angrite parent body from Pb-isotopic data. In Workshop on Chronology of Meteorites and the Early Solar System. Lunar Planet. Inst., Houston, pp. 20–21, LPI Contribution No. 1374.

Amelin Y. and Sapah M. (2012) Cooling rates of plutonic angrites from pyroxene-phosphate U-Pb chronology. *Meteorit. Planet. Sci. Suppl.* **75**, 5199.

Amelin Y., Kaltenbach A. and Stirling C. H. (2011) The U-Pb systematics and cooling rate of plutonic angrite NWA 4590. *Lunar Planet. Sci. Conf.* **42**, 1682.

Brennecka G. A. and Wadhwa M. (2012) $^{238}U/^{235}U$ ratios of angrites: adjusting absolute ages of anchors. *Proc. Natl. Acad. Sci.* **109**(24), 9299–9303.

Brett R., Huebner J. S. and Sato M. (1977) Measured oxygen fugacities on the Angra dos Reis achondrite as a function of temperature. *Earth Planet. Sci. Lett.* **35**, 363–368.

Burns R. G. (1975) Crystal field effects in chromium and its partitioning in the mantle. *Geochim. Cosmochim. Acta* **39**, 857–864.

Connelly J. N., Bizzarro M., Thrane K. and Baker J. A. (2008) The Pb-Pb age of Angrite SAH99555 revisited. *Geochim. Cosmochim. Acta* **72**, 4813–4824.

Crozaz G. and McKay G. (1990) Rare earth elements in Angra dos Reis and Lewis Cliff 86010, two meteorites with similar but distinct magma evolutions. *Earth Planet. Sci. Lett.* **97**, 369–381.

Dohmen R., Chakraborty S. and Becker H.-W. (2002) Si and O diffusion in olivine and implications for characterizing plastic flow in the mantle. *Geophys. Res. Lett.* **29**(21), 2030.

Evans T. M., O'Neill H., St C. and Tuff J. (2008) The influence of melt composition on the partitioning of REEs, Y, Sc, Zr, and Al between forsterite and melt in the system CMAS. *Geochim. Cosmochim. Acta* **72**, 5708–5721.

Faak K., Chakraborty S. and Coogan L. (2013) Mg in plagioclase: experimental calibration of a new geothermometer and diffusion coefficients. *Geochim. Cosmochim. Acta* **123**, 195–217.

Floss C., Crozaz G., McKay G., Mikouchi T. and Killgore M. (2003) Petrogenesis of angrites. *Geochim. Cosmochim. Acta* **67**, 4775–4789.

Glavin D. P., Kubny A., Jagoutz E. and Lugmair G. W. (2004) Mn-Cr isotope systematics of the D'Orbigny angrite. *Meteorit. Planet. Sci.* **39**, 693–700.

Goodrich C. A. (1988) Petrology of the unique achondrite LEW86010. *Lunar Planet. Sci. Conf.* **29**, 399–400.

Greenwood R. C., Franchi I. A., Jambon A. and Buchanan P. C. (2005) Widespread magma oceans on asteroidal bodies in the early Solar System. *Nature* **435**, 916–918.

Heimann M., Parekh P. P. and Herr W. (1974) Comparative study on Al-26 and Mn-53 in eighteen chondrites. *Geochim. Cosmochim. Acta* **38**, 217–234.

Herr W., Herpers U. and Woelfle R. (1972) Study on the cosmic ray produced long-lived Mn-53 in Apollo 14 samples. Proc. Third Lunar Sci. Conf., *Geochim. Cosmochim. Acta*, Suppl. 3, 2, 1763–1769.

Honda M. and Imamura M. (1971) Half-Life of Mn^{53}. *Phys. Rev. C* **4**, 1182–1188.

Hua X., Huss G., Tachibana S. and Sharp T. G. (2005) Oxygen, silicon, and Mn-Cr isotopes of fayalite in the Kaba oxidized CV3 chondrite: Constraints for its formation history. *Geochim. Cosmochim. Acta* **69**, 1333–1348.

Hsu W. (2005) Mn-Cr systematics of pallasites. *Geochem. J.* **39**, 311–316.

Hutcheon I. D., Krot A. D., Keil K., Phinney D. L. and Scott E. R. D. (1998) ^{53}Mn-^{53}Cr dating of fayalite formation in the CV3 chondrite Mokoia: evidence for asteroidal alteration. *Science* **482**, 1865–1867.

Irving A. J. and Kuehner S. M. (2007) Plutonic angrite NWA 4801 and a model for the angrite parent body consistent with petrological and chronological constraints. In Workshop on Chronology of Meteorites and the Early Solar System. Lunar Planet. Inst., Houston, pp. 74–75, LPI Contribution No. 1374.

Ito M. and Ganguly J. (2006) Diffusion kinetics of Cr in olivine and 53Mn-53Cr thermochronology of early solar system objects. *Geochim. Cosmochim. Acta* **70**, 799–809.

Jogo K., Nakamura T., Noguchi T. and Zolotov M. Y. (2009) Fayalite in the Vigarano CV3 carbonaceous chondrite: occurrences, formation age and conditions. *Earth Planet. Sci. Lett.* **287**, 320–328.

Kleine T., Hans U., Irving A. J. and Bourdon B. (2012) Chronology of the angrite parent body and implications for core formation in protoplanets. *Geochim. Cosmochim. Acta* **84**, 186–203.

Kuehner S. M. and Irving A. J. (2007) Grain boundary glasses in plutonic angrite NWA 4590: evidence for rapid decompressive partial melting and cooling on Mercury? *Lunar Planet. Sci. Conf.* **38**, 1522.

Kuehner S. M., Irving A. J., Bunch T. E., Wittke J. H., Hupé G. M. and Hupé A. C. (2006) Coronas and symplectites in plutonic angrite NWA 2999 and implications for Mercury as the angrite parent body. *Lunar Planet. Sci. Conf.* **37**, 1344.

Kurat G., Varela M. E., Brandstätter F., Weckwerth G., Clayton R. N., Weber H. W., Schultz L., Wäsch E. and Nazarov M. A. (2004) Dorbigny: a non-igneous angritic achondrite? *Geochim. Cosmochim. Acta* **68**, 1901–1921.

Latourrette T. and Wasserburg G. J. (1998) Mg diffusion in anorthite: implications for the formation of early solar system planetesimals. *Earth Planet. Sci. Lett.* **158**, 91–108.

Leya I., Wieler R. and Halliday A. N. (2003) The influence of cosmic-ray production on extinct nuclide systems. *Geochim. Cosmochim. Acta* **67**, 529–541.

Ludwig K. R., (2006) ISOPLOT/Ex ver. 3.50. A Geochronological Toolkit for Microsoft Excel.

Lugmair G. W. and Shukolyukov A. (1998) Early solar system timescales according to ^{53}Mn-^{53}Cr systematics. *Geochim. Cosmochim. Acta* **62**, 2863–2886.

Mallmann G. and O'Neill H. St. C. (2009) The crystal/melt partitioning of V during mantle melting as a function of oxygen fugacity compared with some other elements (Al, P, Ca, Sc, Ti, Cr, Fe, Ga, Y, Zr and Nb). *J. Petrol.* **50**, 1765–1794.

Matsuda H., Umemoto S. and Honda M. (1971) Manganese-53 produced by 730 MeV proton bombardment of iron. *Radiochim. Acta* **15**, 51.

McKay G., Crozaz G., Wagstaff J., Yang S.-R. and Lundberg L. (1990) A petrographic, electron microprobe, and ion microprobe study of mini-angrite Lewis Cliff 87051. *Lunar Planet. Sci. Conf.* **21**, 771–772.

McKay G., Lindstrom D., Yang S.-R. and Wagstaff J. (1988) Petrology of unique achondrite Lewis Cliff 86010. *Lunar Planet. Sci. Conf.* **19**, 762–763.

McKay G., Le L., Wagstaff J. and Crozaz G. (1994) Experimental partitioning of rare earth elements and strontium: constraints on petrogenesis and redox conditions during crystallisation of Antarctic angrite Lewis Cliff 86010. *Geochim. Cosmochim. Acta* **58**, 2911–2919.

McKay G. A., Miyamoto M., Mikouchi T. and Ogawa T. (1998) The cooling history of the Lewis Cliff 86010 angrite as inferred from kirschsteinite lamellae in olivine. *Meteorit. Planet. Sci.* **33**, 977–983.

McKibbin S. J., Ireland T. R., Amelin Y., O'Neill H., St C. and Holden P. (2013a) Mn-Cr relative sensitivity factors for Secondary Ion Mass Spectrometry analysis of Mg-Fe-Ca olivine and implications for the Mn-Cr chronology of meteorites. *Geochim. Cosmochim. Acta* **110**, 216–228.

McKibbin S. J., Ireland T. R., Amelin Y., Holden P. and Sugiura N. (2013b) A re-evaluation of the Mn-Cr systematics of olivine from the angrite meteorite D'Orbigny using Secondary Ion Mass Spectrometry. *Geochim. Cosmochim. Acta* **123**, 181–194.

McKibbin S. J., O'Neill H., St C., Mallmann G. and Halfpenny A. (2013c) LA-ICP-MS mapping of olivine from the Brahin and Brenham meteorites: complex elemental distributions in the pallasite olivine precursor. *Geochim. Cosmochim. Acta* **119**, 1–17.

Mikouchi T., Takeda H., Miyamoto M., Ohsumi K. and McKay G. (1995) Exsolution lamellae of kirschsteinite in magnesium-iron olivine from an angrite meteorite. *Am. Mineral.* **80**, 585–592.

Mikouchi T., McKay G. A. and Jones J. H. (2004) Sahara 99555 and D'Orbigny: possible pristine parent magma of quenched angrites. *Lunar Planet. Sci. Conf.* **35**, 1504.

Mikouchi T., McKay G.A., Miyamoto M. and Sugiyama K. (2011a) Olivine xenocrysts in quenched angrites: the first "differentiated" materials in the solar system? Workshop on Formation of the First Solids in the Solar System, held November 7-9, 2011 in Kauai, Hawaii. LPI Contribution No. 1639, p. 9142.

Mikouchi T., Miyamoto M. and McKay G.A. (2011b) Kirschsteinite exsolution lamellae in olivine from young angrites: implications for their thermal histories. Goldschmidt Conference Abstracts, *Mineral. Mag.* 75, 1469.

Mittlefehldt D. W. and Lindstrom M. M. (1990) Geochemistry and genesis of the angrites. *Geochim. Cosmochim. Acta* **54**, 3209–3218.

Mittlefehldt D. W., Killgore M. and Lee M. (2002) Petrology and geochemistry of D'Orbigny, geochemistry of Sahara 99555, and the origin of angrites. *Meteorit. Planet. Sci.* **37**, 345–369.

Mukhopadhyay D. K. and Lindsley D. H. (1983) Phase relations in the join kirschsteinite ($CaFeSiO_4$)-fayalite (Fe2SiO_4). *Am. Mineral.* **68**, 1089–1094.

Nyquist L. E., Shih C. Y., Wiesmann H. and Mikouchi T. (2003) Fossil ^{26}Al and ^{53}Mn in D'Orbigny and Sahara 99555 and the timescale for angrite magmatism. *Lunar Planet. Sci. Conf.* **34**, 1388.

Ogliore R., Huss G. and Nagashima K. (2011) Ratio estimation in SIMS analysis. *Nucl. Instrum. Methods Phys. Res. Sect. B* **269**(17), 1910–1918.

Papike J. J., Karner J. M. and Shearer C. K. (2005) Comparative planetary mineralogy: valence state partitioning of Cr, Fe, Ti, and V among crystallographic sites in olivine, pyroxene, and spinel from planetary basalts. *Am. Mineral.* **90**, 277–290.

Petry C., Chakraborty S. and Palme H. (2004) Experimental determination of Ni diffusion coefficients and their dependence on temperature, composition, oxygen fugacity, and crystallographic orientation. *Geochim. Cosmochim. Acta* **68**, 4179–4188.

Prinz M., Keil K., Hlava P. F., Berkley J. L., Gomes C. B. and Curvello W. S. (1977) Studies of Brazilian Meteorites, III. Origin and history of the Angra dos Reis achondrite. *Earth Planet. Sci. Lett.* **35**, 317–330.

Sanborn M. E., Carlson R. W. and Wadhwa M. (2011) ^{147,146}Sm-^{143,142}Nd and ^{87}Rb-^{87}Sr systematics of the angrites Northwest Africa 4590, Northwest Africa 4801, and D'Orbigny. *Lunar Planet. Sci.* **42**, 2369.

Shukolyukov A. and Lugmair G. W. (2007) The Mn-Cr isotope systematics of bulk angrites. *Lunar Planet. Sci. Conf.* **38**, 1423.

Shukolyukov A. and Lugmair G. W. (2008) Mn-Cr chronology of eucrite CMS 04049 and angrite NWA 2999. *Lunar Planet. Sci. Conf.* **39**, 2094.

Shukolyukov A., Lugmair G. W. and Irving A. J. (2009) Mn-Cr isotope systematics of angrite Northwest Africa 4801. *Lunar Planet. Sci. Conf.* **40**, 1381.

Spandler C. and O'Neill H. St. C. (2010) Diffusion and partition coefficients of minor and trace elements in San Carlos olivine at 1,300°C with some geochemical implications. *Contrib. Miner. Petrol.* **159**, 791–818.

Spivak-Birndorf L., Wadhwa M. and Janney P. (2009) ^{26}Al-^{26}Mg systematics in D'Orbigny and Sahara 99555 angrites: implications for high-resolution chronology using extinct chronometers. *Geochim. Cosmochim. Acta* **73**, 5202–5211.

Sugiura N., Miyazaki A. and Yanai K. (2005) Widespread magmatic activities on the angrite parent body at 4562 Ma ago. *Earth Planets Space* **57**, e13–e16.

Taura H., Yurimoto H., Kurita K. and Sueno S. (1998) Pressure dependence on partition coefficients for trace elements between olivine and coexisting melts. *Phys. Chem. Minerals* **25**, 469–484.

Tonui E. K., Ngo H. H. and Papanastassiou D. A. (2003) Rb-Sr and Sm-Nd study of the D'Orbigny angrite. *Lunar Planet. Sci. Conf.* **34**, 1812.

Treiman A.H. (1989) An alternate hypothesis for the origin of Angra dos Reis: porphyry, not cumulate. In Proceedings of the 19th *Lunar Planet. Sci. Conf.*, pp. 443–450.

Vockenhuber C., Oberli F., Bichler M., Ahmad I., Quitté G., Meier M., Halliday A. N., Lee D. C., Kutschera W., Steier P., Gehrke R. J. and Helmer R. G. (2004) New half-life measurement of ^{182}Hf: improved chronometer for the early solar system. *Phys. Rev. Lett.* **93**, 172501.

Wadhwa M. (2008) Redox conditions on small bodies, the Moon and Mars. *Rev. Mineral. Geochem.* **68**, 493–510.

Warren P. H. and Kallemeyn G. W. (1995) Angrites: a volatile-rich variety of asteroidal basalt (except for alkalies and gallium!). *Meteoritics* **30**, 593.

Woelfle R., Herr W. and Herpers U. (1973) Determination of the activation cross-section σ_{therm} and of the half-life of ^{53}Mn by a 587 days reactor irradiation. *Radiochim. Acta* **18**, 207–211.

Yamaguchi A., Mikouchi T., Ito M., Shirai N., Barrat J. A., Messenger S. and Ebihara M. (2013) Experimental evidence of

fast transport of trace elements in planetary basaltic crusts by high temperature metamorphism. *Earth Planet. Sci. Lett.* **368**, 101–109.

Yin Q.-Z., Amelin Y. and Jacobsen B. (2009) Project milestones: testing consistent chronologies between extinct ^{53}Mn-^{53}Cr and extant U-Pb systematics in the early solar system. *Lunar Planet. Sci. Conf.* **40**, 2060.

Associate editor: Maud Boyet